Cell membrane and gold nanoparticles effects on optical immersion experiments with noncancerous and cancerous cells: finite-difference time-domain modeling

Stoyan Tanev
Carleton University
Department of Systems and Computer Engineering
Ottawa, Ontario, Canada

Valery V. Tuchin
Saratov State University
Institute of Optics and Biophotonics
Saratov, 410012 Russia

Paul Paddon
Lumerical Solutions, Inc.
Vancouver, British Columbia, Canada

Abstract. Pilot results on the application of the finite-difference time-domain (FDTD) approach for studying the implementation of the optical immersion technique for the visualization of single and multiple gold nanoparticles in biological cells are presented. We focus on two different scenarios considering single biological cells containing (1) cytoplasm, nucleus, and membrane and (2) cytoplasm, nucleus, gold nanoparticles, and membrane. To the best of our knowledge, this is the first time the cell membrane thickness and gold nanoparticle effects on the forward scattered light from biological cells are discussed. The applicability and the potential of the FDTD approach for studying optical immersion technique enhanced bioimaging is demonstrated. © 2006 Society of Photo-Optical Instrumentation Engineers. [DOI: 10.1117/1.2400239]

Keywords: biological cell; finite-difference time domain; gold nanoparticles; surface plasmon resonance; light scattering; immersion technique.

Paper 06121LRRR received May 17, 2006; revised manuscript received Sep. 19, 2006; accepted for publication Sep. 20, 2006; published online Dec. 13, 2006.

The development of noninvasive optical methods for biomedical diagnostics requires a fundamental understanding of how light scatters from normal and pathological structures within biological tissues.[1,2] Unfortunately, the biological origins of the differences in the light scattering patterns from noncancerous and pathological (i.e., precancerous) cells and tissues are not fully understood. In many biomedical and photonics micro- and nanostructure research studies optical software simulation and modeling tools are the only means to get a deeper understanding, or any understanding at all, of the underlying physical and biochemical processes. Some of the numerical modeling approaches that can be used for the modeling of the light scattering from biological cells have been recently summarized[3] and include the finite-difference time-domain (FDTD) method.[4–8] Advances in using the FDTD method to study the effect of nanometer-scale features embedded within micrometer-scale particles were also recently reviewed.[9] The FDTD approach was first adopted as a better alternative of Mie theory and has now been acknowledged as a powerful tool for studying the nature of the light-scattering mechanisms from biological cells during the detection of early changes associated with the dysplasia-to-carcinoma sequence, including increased nuclear size, nuclear pleomorphism, and nuclear-to-cytoplasmic ratio.[6]

Recently we demonstrated the applicability of the FDTD approach to numerically study the effect of the optical immersion technique (OIT) for enhancing the light-scattering images of biological cells.[8] We demonstrated for the first time that taking into account the finite thickness of the cell membrane is critically important for the correct modeling of the optical clearing effect. In this letter, we apply the FDTD modeling technique to provide additional insight on the effect of the cell membrane thickness in OIT experiments to enhance phase contrast microscope imaging. We also provide initial simulation results on the implementation of the OIT for the visualization of gold nanoparticles in biological cells. The presented results extend the applicability of the FDTD approach to new and promising biomedical optics research areas such as enhanced bioimaging using OIT.

The OIT is based on the so called "optical clearing" (OC) effect consisting in the increased light transmission through microbiological objects due to the matching of the refractive indices (RIs) of some of their morphological components to that of the extracellular medium. It was first applied in the 1950s to cell and microorganism phase contrast microscopy studies.[10,11] In the last decade, it has greatly regained its popularity and can be now considered as a promising tool in biomedical optics research.[12] The OIT can be most easily demonstrated by analyzing phase-contrast microscope images of bacterial cells containing only a cytoplasm and a membrane.[11] In the case where refractive indices of cell cytoplasm n_1 and extracellular space n_{ex} are equalized, $n_1 = n_{ex}$, and due to the extremely small thickness of the cell membrane, the optical path accumulated by the light rays going through the cell parts free of organelles and extracellular space is almost the same and much smaller than the optical path of the light ray going along the cell membrane. Some light rays accumulate an additional phase shift due to the RI difference of the organelle. If the RI of the extracellular fluid is externally controlled by the administration of an appropriate chemical agent, the visual

Address all correspondence to Stoyan Tanev, 4456 Mackenzie Building, 1125 Colonel By Drive, Ottawa, Ontario, Canada K1S 5B6; Tel: (613) 520-2600 x1894; E-mail: tanev@sce.carleton.ca
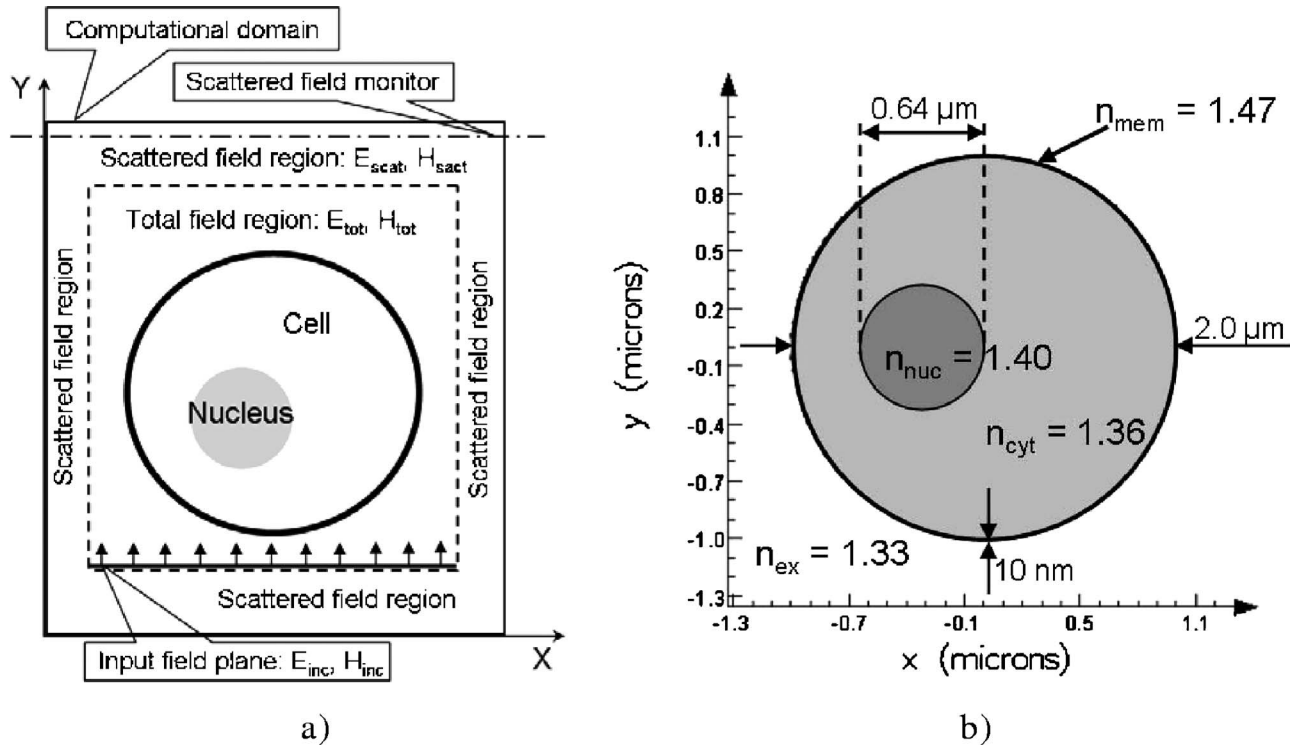
Fig. 1 (a) Schematic representation of the total field/scattered field FDTD formulation and (b) cell RI distribution and geometry.

disappearing of the cytoplasm and the sharp enhancement of the membrane brightness can be used as a way for measuring the RI of the cytoplasm using phase microscopy.[11]

The FDTD technique is a numerical solution of Maxwell's equations.[13,14] The FDTD numerical scheme is applied on a finite in space and time numerical equivalent of the physical reality under investigation, which, in our case, is a biological cell immersed in a host material. The finite dimensions of the computational domain require the application of appropriate absorbing boundary conditions (ABCs). The ABCs are used to truncate the computational domain and absorb any simulated wave reaching its boundaries as if it were to potentially propagate to infinity according to the particular physical properties of the host medium.[14]

In light scattering simulation experiments one uses the so-called total-field/scattered-field (TFSF) formulation[8,14] to excite the magnetic and electric fields and simulate a linearly polarized plane wave propagating in a finite region of a homogeneous absorptive dielectric medium. A schematic representation of the 2-D FDTD computational domain is shown in Fig. 1(a). TFSF sources are used to separate the computation region into two distinct regions. The first [dashed line rectangle in Fig. 1(a)] contains the total near fields $E_{tot}=E_{inc}+E_{scat}$ and $H_{tot}=H_{inc}+H_{scat}$, i.e., the sum of the incident field and the scattered near field. The second region (outside of the dashed line rectangle) contains only the scattered near fields $E_{scat}=E_{tot}-E_{inc}$ and $H_{scat}=H_{tot}-H_{inc}$. The TFSF source is particularly useful to study the scattering behavior of objects, as the scattered near field data can be isolated from the incident field and further postprocessed to acquire as much useful information as possible. In Fig. 1(a) a TFSF ideal plane wave is injected along the lower edge of the total field region in the

upward direction. Everything inside the TFSF boundary (the dashed line rectangle) is total near field, while everything outside is only scattered near field. Thus, in the absence of any objects, the wave propagates within the TFSF region and is subtracted out at the other end; this of course results in no scattered field at all. However, if one places an object in the path of the TFSF plane wave, this introduces scattered fields that then propagate outside the total field area. Consequently, one can then measure the total or scattered transmission, by placing monitors inside or the outside of total field region, respectively. Since these are the near fields that are measured, an additional analysis of the results may (but not necessarily) require a postprocessing numerical procedure to transform the near fields into their far-field counterparts. At the edges, the entire FDTD computational domain is truncated by the so-called uniaxial perfectly matched boundary conditions.[8,14]

The simulation results presented here were performed by the FDTD Solutions™ software,[15] where all the features of the FDTD scheme already described are built into the graphical user interface. The forward scattered light field from single biological cells is of particular interest here since it is its phase—the phase accumulated due to the RI variations by a plane wave propagating through the cell—that is mostly relevant for phase contrast microscope imaging. The phase contrast technique translates small variations in phase into corresponding changes in amplitude, which can be visualized as differences in image contrast. Advanced versions of quantitative phase microscopy have been reported to translate forward-scattered optical phase information into nanometer-scale-resolution cell images.[16] The simulation framework presented here could be applied to provide valuable insights for further development of such new imaging techniques. Insights
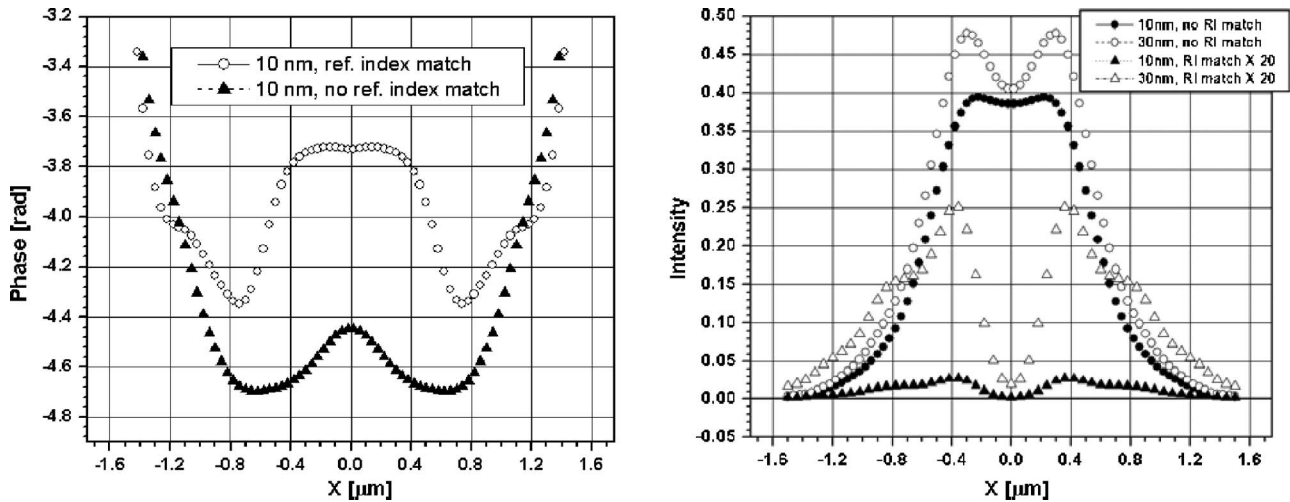
Fig. 2 The 2-D phase (left) and intensity (right) distribution of the forward scattered near field ($E_{x,\text{scat}}$ component) from a cell without nucleus with parameters: $n_{\text{ex}}=1.33$ (no RI match), $n_{\text{ex}}=1.36$ (RI match), membrane thicknesses 10 nm and 30 nm. In the case of RI matching, the intensity values are multiplied by a factor of 20.

from the analysis of the forward-scattered field will be also highly relevant when studying the light-scattering properties of very fine features and nanoparticles in cells by means of conventional microscopes appropriately set up to operate in a dark image collection mode where the center of the illuminating beam is blocked from entering the light collection cone and a bright image on a dark background is formed due the scattered light only.[17]

Since the cell membrane thickness is of the order of 10 nm, any 3-D FDTD simulation will require a very fine numerical resolution (much below the limit ensuring the numerical stability of the algorithm) leading to heavy, computationally intensive and time-consuming numerical experiments. This motivated us to proceed with a series of 2-D TE FDTD simulations to analyze the transverse distribution (along the x coordinate axe and perpendicular to the direction of propagation which is along the $+y$ coordinate axe) of the three nonzero components ($E_{x,\text{scat}}, E_{y,\text{scat}}, H_{z,\text{scat}}$) of the forward scattered near field at a location schematically represented by the scattered near field monitor shown in Fig. 1(a). The most general case of cell geometry is shown in Fig. 1(b) together with the specific values of the RIs of its morphological components: cytoplasm, nucleus, extracellular medium, and membrane.[18–20] In all the simulation scenarios described in this letter the 2-D FDTD computational domain has dimensions 3×3 μm. The resolution in both the x and y directions is 2 nm. The time step is 0.00235865 fs. The simulation time is 500 fs. The total field region [see Fig. 1(a)] is 2.8 $\times 2.8$ μm large and located right in the middle of the computational domain. The incident plane wave ($\lambda=632.8$ nm) is launched at the lower edge ($y=-1.4$ μm) of the total field region and propagates in the $+y$ direction. The forward-scattered E_x near-field component (the major nonzero field component of the TE propagation case) is saved at the end of the simulation in the scattered field region by means of a scattered field monitor [see Fig. 1(b)] located at $y=1.448$ μm.

Figure 2 presents the FDTD simulation results for the

transverse phase and intensity distributions of the forward-scattered $E_{x,\text{scat}}$ field component. The morphology of the cell is as the one shown in Fig. 1(b) but without the nucleus. The analysis of the simulation results shows that the phase and the intensity of the forward-scattered light are sensitive to cell membrane thickness. This sensitivity is more clearly visible in the intensity distribution (Fig. 2, right) where a 10- to 30-nm increase in the cell membrane thickness leads to $\sim$1.18 times (no RI matching) and to $\sim$10 times (RI matching) increase the maximum intensity values. The OC effect due to the RI matching of the cytoplasm and the extracellular medium is clearly visible on both the phase (Fig. 2, left) and the intensity distributions (Fig. 2, right). The RI matching leads to a drastic decrease of the maximum forward-scattered light intensity ($\sim$250 times!) and a sharper phase contrast of the forward-scattered near-field symmetrically located on both sides (left and right) of a plane going through the cell center. To the best of our knowledge, this is the first rigorous numerical modeling study demonstrating this enhancement of the cell membrane phase contrast at optical immersion conditions. Note that the maximum phase contrast does appear at $\sim$0.742 μm from the center of the phase distribution and not at approximately 1 μm, corresponding to the location of the cell membrane. The 3-D FDTD simulations showed that the exact transverse location of the maximum phase contrast depends on the polarization of the incident light.[8] The details of these dependences represent a significant interest and will be further investigated in future studies.

The analysis of the results of the 2-D FDTD simulation for the cell with nucleus (Fig. 3) can be used to draw several conclusions. The presence of the nucleus introduces an additional optical phase accumulation on the forward-scattered near-field component $E_{x,\text{scat}}$, leading to an asymmetric transverse distribution of its phase and intensity. The influence of the nucleus is very small for the unmatched case and very strong for the matched case. This behavior is intuitively clear since, at immersion conditions, the optical phase accumulation is driven by both, the specific size of the nucleus and the
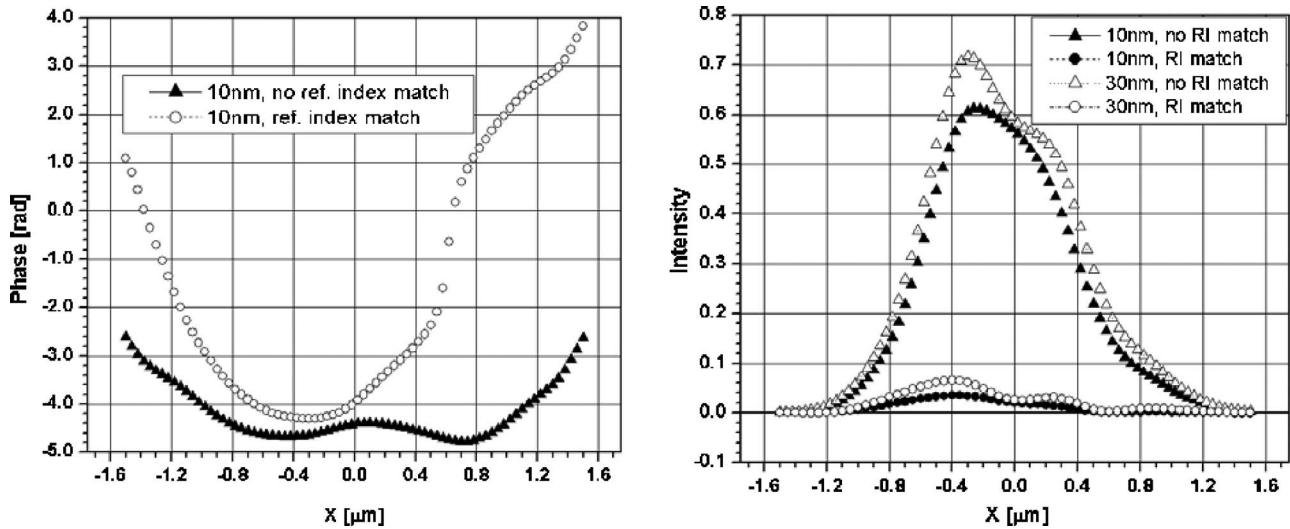
Fig. 3 Effect of optical immersion on the phase and intensity of the forward-scattered near-field (TE case, $E_{x,\text{scat}}$ component) from a cell with a nucleus [for parameters see Fig. 1(b)]. Transverse phase (left) and intensity (right) distributions for both cases—with and without RI matching. Right-hand graph shows the effect of cell membrane thickness: 10 versus 30 nm. The membrane of the nucleus is not taken into account.

associated RI contrast: 1.40 (nucleus) to 1.36 (cytoplasm). As in the previous case of a cell without a nucleus, the OC effect enhances the effect of the finite membrane thickness on the intensity of the forward-scattered light—the ratio between the maximum forward scattered light intensities corresponding to cell membrane thicknesses 30 and 10 nm increases from approximately 1.16 (no RI matching) to 1.86 (RI matching). The variation of the finite membrane thickness leads to small relative changes of the phase and intensity distributions on top of the contributions due to the nucleus.

Gold nanoparticles exhibit the ability to resonantly scatter visible and near-IR light. This property is the result of the excitation of surface plasmon resonances (SPRs) and is extremely sensitive to the size, shape, and aggregation state of the particles.[21–23] The ability to resonantly scatter visible and near-IR light is currently being explored for vital microscopy in living specimens.[24] In this letter, we examine the applicability of the FDTD modeling approach to study the effect of gold nanoparticles presence on the forward-scattered near light field from single biological cells at optical immersion conditions. We used the dispersion model for gold derived from the experimental data provided by Johnson and Christy.[25] More details on the gold optical material properties model are presented elsewhere.[26]

The simulation results are shown in Fig. 4. The configurations of our numerical experiment was inspired by a recently published research study.[17] We modeled two different scenarios. In the first scenario (case a) the gold nanoparticles are randomly distributed in the cytoplasm with a 2-D density of 15.29 nanoparticles/μm^2 and no particles in the nucleus. In our simulations, case a corresponds to both cancerous and noncancerous cells. El-Sayed et al. report that there are slight differences of the nanoparticle distributions in the cytoplasm of noncancerous and cancerous cells (spotted pattern versus a more homogeneous distribution, respectively). However, we did not find enough quantitative information that could be used to design two different nanoparticle configurations. In the second scenario (case b), we consider the antiepidermal

growth factor receptor (anti-EGFR) antibody conjugated gold nanoparticles as attached to the cell membrane (on both the internal and external side of the cell) with a linear density of 3.5 nanoparticles/μm. This scenario corresponds to cancerous cells only. El-Sayed et al.[17] report that anti-EGFR gold conjugates are located on the external side of the cytoplasmic membrane. We intentionally located the nanoparticles on both sides of the membrane based on the fact that the 2-D approximation of the 3-D cancer cell geometry makes some of the anti-EGFR anti-body conjugated nanoparticles appear as being located inside the cell in the proximity of the membrane.[26] A rigorous approach would require the implementation of 3-D cell geometry/FDTD models and will be considered in future studies.

For comparison we also show the results for the situation (case c) where the cell does not contain gold nanoparticles. The slight change of the optical properties of gold nanoparticles due to the anti-EGFR antibody conjugation[17] is not taken into account. The conjugation effect is taken into account through the different positioning of the nanoparticles within the cell, i.e., in the proximity of the cell membrane.

The analysis of the simulation results demonstrates the positive effect of the OC for the phase contrast enhancement of biological cells containing nanoparticles. In both cases, with and without RI matching, the phase distribution of the forward scattered near field reveals a complex variation in the direction perpendicular to the direction of propagation. This is due to the cumulative effect of the microscopic absorbing and scattering phenomena associated with the randomly distributed gold nanoparticles. We used 2-D FDTD simulations of light scattering from a single gold nanoparticle to find out that, at $\lambda = 632.8$ nm, its scattering cross section is two times larger than the absorbing one indicating that the phase accumulation is predominantly due to scattering effects. The random distribution of the gold nanoparticles within the cell cytoplasm (case a) leads to a larger maximum phase accumulation as compared to case b—random distribution of
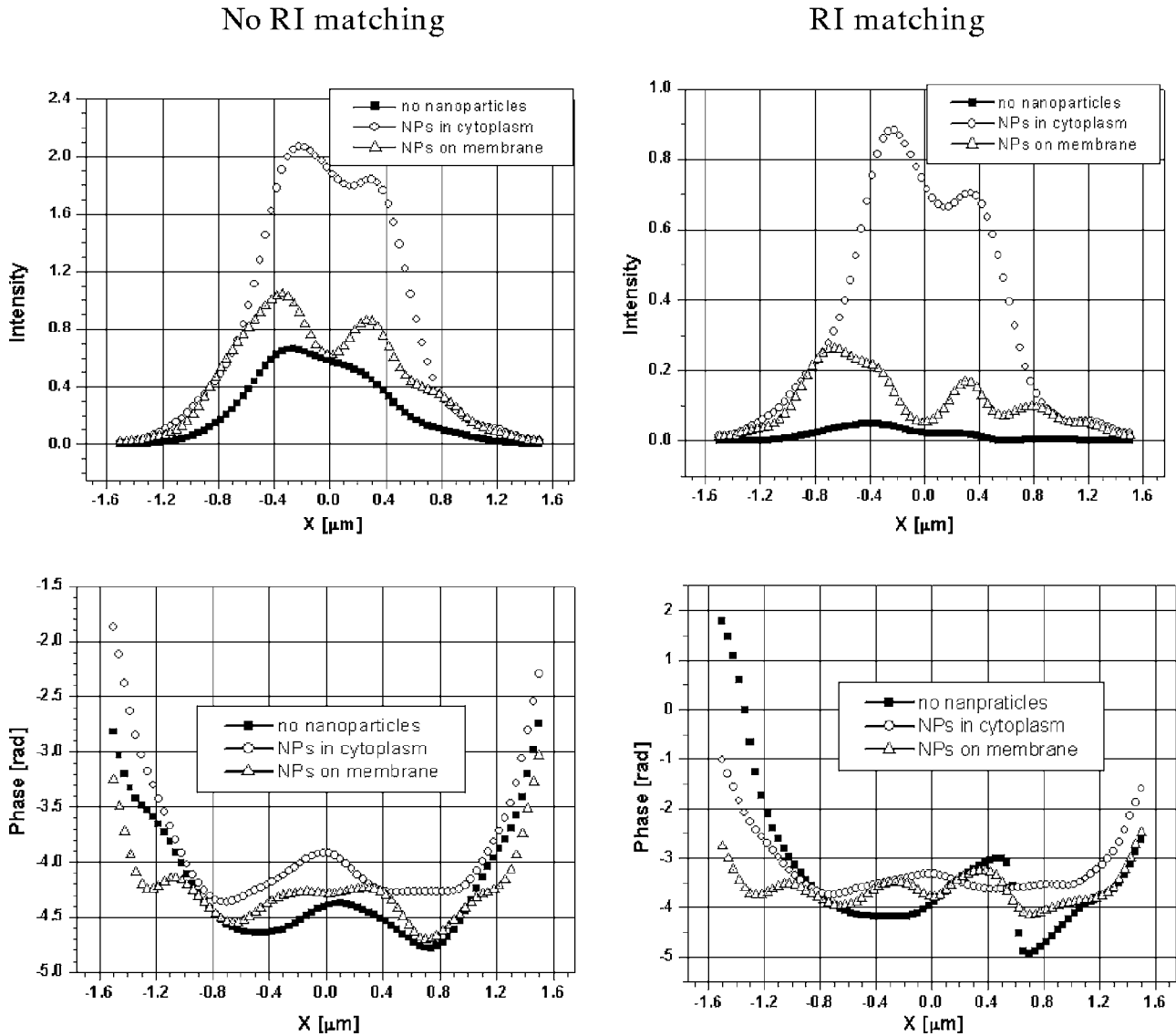
No RI matching

RI matching

Fig. 4 Intensity and phase distributions of the forward-scattered light (near) field (TE case, $E_{x,scat}$ component) from biological cells containing multiple gold nanoparticles with optical properties described in Ref. 18 and a diameter of 40 nm: (a) ○, gold nanoparticles randomly distributed in the cytoplasm; (b) △, gold nanoparticles randomly distributed on the internal side of the membrane; and (c) ■, no gold nanoparticles in the cell.

the gold nanoparticles in the proximity of the cell membrane. The transverse distribution of the optical intensity is more revealing. It shows that at optical immersion conditions (RI matching) there is a ~2.4 times decrease in the maximum intensity of the forward scattered near field, however, this maximum intensity is ~14.8 times (case a) and ~4.5 times (case b larger relative to case c). In the no RI matching case, the corresponding values are ~3.2 (case a) and ~1.62 (case b).

Note that the complex variation of the forward scattered phase distributions should be studied in more details by considering (1) larger cell sizes, (2) the effect of nucleus size on light-scattering intensity, (3) light-scattering intensity as a function of gold nanoparticle density, and (4) the effect of localized clusters of nanoparticles. The simulation results show the potential of the FDTD approach for studying all

those effects. They have a pilot character and provide a motivation for further research.

We applied the FDTD modeling technique to study the effect of the cell membrane thickness in optical-immersion-based light-scattering experiments within a context that is highly relevant for phase contrast microscope imaging. The effect of the cell membrane thickness is of particular interest for smaller cells without a nucleus where the membrane thickness, depending on cell type (bacteria or other microbiological structures), could show a high degree of variability (10 to 100 nm). This influenced the particular choice of (relatively small) cell dimensions used in the simulations. The scope of the study was extended then to account for the presence of organelles (the nucleus) and gold nanoparticles by keeping the bacteria-like results as a reference. Given the pilot nature of the study, we found this particular choice to be a

reasonable compromise. The computational approach, however, is perfectly applicable to larger cell sizes. Simulation studies including larger cell dimensions are underway and the results will be published elsewhere.

We provided preliminary results on the application of the FDTD approach for studying the implementation of the OIT for the enhanced imaging of gold nanoparticles in biological cells. In spite of the relatively small cell size, the results would be of relevance for the interpretation of light-scattering experiments from cancerous cells where the application of gold nanoparticle imaging is very promising. Three different scenarios are considered involving biological cells containing (1) cytoplasm and membrane; (2) cytoplasm, nucleus, and membrane; and (3) cytoplasm, nucleus, gold nanoparticles, and membrane. To the best of our knowledge, this is the first research study discussing the cell membrane thickness and gold nanoparticle effects on the forward-scattered near field from biological cells. The analysis of the simulation results shows that, in all cases, the scattering properties of the cell are visibly controlled at optical immersion. The FDTD modeling approach is shown to be a very powerful tool for the study of OIT-enhanced nanobiophotonics imaging.

References

1. P. N. Prasad, "Bioimaging: principles and techniques," Chap. 7 in *Introduction to Biophotonics*, pp. 203–249, John Wiley & Sons, Hoboken, NJ (2003).
2. V. V. Tuchin, *Tissue Optics: Light Scattering Methods and Instruments for Medical Diagnosis*, SPIE Tutorial Texts in Optical Engineering, Vol. TT38, Bellingham, WA (2000).
3. F. M. Kahnert, "Numerical methods in electromagnetic scattering theory," *J. Quant. Spectrosc. Radiat. Transf.* **73**, 775–824 (2003).
4. R. Drezek, A. Dunn, and R. Richards-Kortum, "A pulsed finite-difference time-domain (FDTD) method for calculating light scattering from biological cells over broad wavelength ranges," *Opt. Express* **6**, 147–157 (2000).
5. T. Tanifuji and M. Hijikata, "Finite difference time domain (FDTD) analysis of optical pulse responses in biological tissues for spectroscopic diffused optical tomography," *IEEE Trans. Med. Imaging* **21**, 181–184 (2002).
6. R. Drezek, M. Guillaud, T. Collier, I. Boiko, A. Malpica, C. Macaulay, M. Follen, and R. R. Richards-Kortum, "Light scattering from cervical cells throughout neoplastic progression: influence of nuclear morphology, DNA content, and chromatin texture," *J. Biomed. Opt.* **8**, 7–16 (2003).
7. S. Tanev, W. Sun, R. Zhang, and A. Ridsdale, "Simulation tools solve light-scattering problems from biological cells," *Laser Focus World* **40**(1), 67–70 (2004).
8. S. Tanev, W. Sun, N. Loeb, P. Paddon, and V. V. Tuchin, "The finite-difference time-domain method in the biosciences: modelling of light scattering by biological cells in absorptive and controlled extra-cellular media," in *Advances in Biophotonics, NATO Science Series I*, Vol. **369**, B. C. Wilson, V. V. Tuchin, and S. Tanev, Eds., pp. 45–78, IOS Press, Amsterdam (2005).
9. X. Li, A. Taflove, and V. Backman, "Recent progress in exact and reduced-order modeling of light-scattering properties of complex structures," *IEEE J. Sel. Top. Quantum Electron.* **11**, 759–765 (2005).
10. R. Barer, K. F. A. Ross, and S. Tkaczyk, "Refractometry of living cells," *Nature (London)* **171**, 720–724 (1953).
11. B. A. Fikhman, *Microbiological Refractometry*, Medicine, Moscow (1967).
12. V. V. Tuchin, *Optical Clearing of Tissues and Blood*, Vol. PM 154, SPIE Press, Bellingham, WA (2005).
13. W. Sun, N. G. Loeb, S. Tanev, and G. Videen, "Finite-difference time-domain solution of light scattering by an infinite dielectric column immersed in an absorbing medium," *Appl. Opt.* **44**, 1977–1983 (2005).
14. A. Taflove and S. Hagness, *Computational Electrodynamics: The Finite-Difference Time Domain Method*, 3rd ed., Artech House, Boston (2005).
15. The FDTD Solutions™ was developed by Lumerical Solutions Inc., Vancouver, BC, Canada, www.lumerical.com.
16. G. Popescu, T. Ikeda, C. Best, K. Badizadegan, R. Dasari, and M. Feld, "Erythrocyte structure and dynamics quantified by Hilbert phase microscopy," *J. Biomed. Opt.* **10**, 06503 (2005).
17. I. H. El-Sayed, X. Huang, and M. A. El-Sayed, "Surface plasmon resonance scattering and absorption of anti-EGFR antibody conjugated gold nanoparticles in cancer diagnostics: applications in oral cancer," *Nano Lett.* **5**, 829–834 (2005).
18. R. Barer and S. Joseph, "Refractometry of living cells," *Q. J. Microsc. Sci.* **95**, 399–423 (1954).
19. A. Brunsting and P. Mullaney, "Differential light scattering from spherical mammalian cells," *Biophys. J.* **14**, 439–453 (1974).
20. I. Vitkin, J. Woolsey, B. Wilson, and R. Anderson, "Optical and thermal characterization of natural (sepia oficinalis) melanin," *Photochem. Photobiol.* **59**, 455–462 (1994).
21. J. Yguerabide and E. Yguerabide, "Light-scattering submicroscopic particles as highly fluorescent analogs and their use as tracer labels in clinical andbiological applications," *Anal. Biochem.* **262**, 137–156 (1998).
22. N. G. Khlebtsov, A. G. Melnikov, V. A. Bogatyrev, and L. A. Dykman, "Optical properties and biomedical applications of nanostructures based on gold and silver bioconjugates," in *Photopolarimetry in Remote Sensing*, G. Videen, Ya. S. Yatskiv, and M. I. Mishchenko, Eds., pp. 265–307, Kluwer Academic, Dordrecht (2004).
23. V. P. Zharov, J.-W. Kim, D. T. Curiel, and E. Maaike, "Self-assembling nanoclusters in living systems: application for integrated photothermal nanodiagnostics and nanotherapy," *Nanomed. Nanotechnol., Biol. Med.* **1**, 326–345 (2005).
24. K. Sokolov, M. Follen, J. Aaron, I. Pavlova, A. Malpica, R. Lotan, and R. Richards-Kortum, "Real time vital imaging of pre-cancer using anti-EGFR antibodies conjugated to gold nanoparticles," *Cancer Res.* **63**, 1999–2004 (2003).
25. P. B. Johnson and R. W. Christy, "Optical constants of noble metals," *Phys. Rev. B* **6**, 4370–4379 (1972).
26. S. Tanev, V. V. Tuchin, and P. Paddon, "Light scattering effects of gold nanoparticles in cells," *Laser Phys. Lett.* **3**(12), 594–598 (2006).